By choosing the atomic system and the frequency of the control laser appropriately, it should be possible to control beams from the far-infrared to the vacuum ultraviolet. The rotation effect also provides a sensitive technique for measuring two-photon cross sections. Extensions of this work to other schemes which use the two-photon dispersion to provide pulse compression and reshaping are presently under investigation.

The authors acknowledge many helpful and stimulating conversations with J. E. Bjorkholm and thank C. K. N. Patel for a critical reading of the manuscript. The technical assistance of W. N. Leibolt is also gratefully acknowledged.

[1]See, for example, F. Biraben, B. Cagnac, and G. Grynberg, Phys. Rev. Lett. 32, 643 (1974); M. D. Levenson and N. Bloembergen, Phys. Rev. Lett. 32, 645 (1974); T. W. Hänsch, S. A. Lee, R. Wallenstein, and C. Wieman, Phys. Rev. Lett. 34, 307 (1975); W. K. Bischel, P. J. Kelley, and C. K. Rhodes, Phys. Rev. Lett. 34, 300 (1975).

[2]R. H. Lehmberg, J. Reintjes, and R. C. Eckhardt, Appl. Phys. Lett. 25, 374 (1974).

[3]D. Grischkowsky, Phys. Rev. Lett. 24, 866 (1970).

[4]J. E. Bjorkholm and A. Ashkin, Phys. Rev. Lett. 32, 129 (1974).

[5]H. M. Gibbs, G. G. Churchill, and G. J. Salamo, Opt. Commun. 12, 396 (1974).

[6]A. M. Bonch-Bruevich, N. N. Kostin, and V. A. Khodovoi, Zh. Eksp. Teor. Fiz., Pis'ma Red. 3, 279 (1966) [JETP Lett. 3, 279 (1966)].

[7]D. Grischkowsky, Appl. Phys. Lett. 25, 566 (1974).

[8]M. T. Loy, Appl Phys. Lett. 26, 99 (1974).

[9]J. E. Bjorkholm, E. H. Turner, and D. B. Pearson, Appl. Phys. Lett. 26, 564 (1975).

[10]B. Cagnac, G. Grynberg, and F. Biraben, J. Phys. (Paris) 34, 845 (1973).

[11]J. E. Bjorkholm and P. F. Liao, Phys. Rev. Lett. 33, 128 (1974).

[12]R. H. Stolen and A. Ashkin, Appl. Phys. Lett. 22, 294 (1972).

Magnetic Braiding Due to Weak Asymmetry*

Alexander B. Rechester and Thomas H. Stix
Plasma Physics Laboratory, Princeton University, Princeton, New Jersey 08540
(Received 5 August 1975)

Magnetic surfaces for a plasma with a helical current perturbation $\sim \epsilon^2$ are destroyed by toroidal effects or by a second current perturbation, of incommensurate helicity, and the behavior of magnetic field lines becomes stochastic in layers of relative width $\epsilon^{-l} \times \exp(-\pi/2\epsilon)$, where $l \simeq 2|m_1/m| + 1$ with m and m_1 the azimuthal mode numbers of the original helical field and of the perturbation.

This work considers how the magnetic surfaces for a tokamak discharge are affected by helical perturbations of the plasma current. Such current perturbations are known to be associated with resistive modes,[1,2] and substantial experimental evidence has been offered[3] for the occurrence of magnetic islands[4] associated with nonlinear tearing instabilities.[5,6] In this paper we show that the existence of two such modes with different helicity *or* the effect of toroidal geometry on a single such mode leads to the destruction of magnetic surfaces. The resultant stochastic wandering or "braiding" of the magnetic lines can produce collisionless radial heat transport, enhanced current penetration, and radial particle transport, and may change the inductance for toroidal plasma current flow so that sudden onset of braiding would produce negative or positive spikes in the loop-voltage signal.[7]

The mechanism of magnetic-surface destruction[8] was first investigated in two classic papers on magnetic irregularities,[9,10] where it was demonstrated that a spectrum of overlapping resonances produces stochastic wandering of the magnetic field lines. In this work we start with a field of helical symmetry and exact magnetic surfaces which exhibits a single set of primary islands, i.e., a single resonance at some $r = r_0$ between the helical variation and the rotational transform $\iota(r)$. Weak asymmetry is introduced via a first-order magnetic perturbation of different helicity which might be due to toroidal effects or to the presence of a second magnetic resonance at $r = r_1$. The incommensurate perturbation is found to produce little *secondary* islands which appear wherever the Fourier components of the perturbation resonate with the *local* transform, $\omega(k)$, Eq. (4), within the *primary* islands.

In fact, a pileup occurs with a denumerable infinity of chains of these little secondary islands appearing as the primary separatrix is approached from both inside and outside. Calculating the width of the secondary islands in each such chain and the spacing between adjacent chains, we find that the relative thickness of the braiding region, within which secondary-island overlap occurs (see Fig. 1), is given by a nonanalytic function of the expansion parameter, ϵ, namely, $\epsilon^{-l}\exp(-\pi/2\epsilon)$. ϵ, defined in Eq. (8), is proportional to the thickness of the primary islands and is inversely proportional to $m_1|r_1-r_0|/m$. l is approximately $2|m_1/m|+1$, and m and m_1 are azimuthal mode numbers for the original helical field and for the perturbation, respectively. This result may be compared with an earlier estimate[11] for the thickness of the stochastic layer, $\sim\exp(-1/\epsilon)$. We also find that toroidal effects produce stochastic regions around the separatrices associated with any magnetic island. As a specific illustration, we consider the $m=2$ ST tokamak islands, measured by von Goeler,[3] and evaluate the fraction of island area in which the magnetic field is stochastic.

It is worth noting that the results obtained here may be directly applied also to the analysis of the motion of a charged particle in the field of two incommensurate plane waves.[11]

We consider, in zero order, a magnetic field of helical symmetry, $\vec{B}(r,u)$, $u\equiv m\theta-nz/R$. r, θ, and z are the usual cylindrical coordinates. The field is derivable from a vector potential, $\vec{B}=\nabla\times\vec{A}(r,u)$, and direct substitution will verify that the flux function[12] $\psi=mA_z+n(r/R)A_\theta=-\int[mB_\theta-(nr/R)B_z]dr$ satisfies the condition for a magnetic surface, $\vec{B}\cdot\nabla\psi=0$. We define $2\pi/\iota(r)\equiv q(r)\equiv r\langle B_z\rangle/R\langle B_\theta\rangle$, where the averages are taken over a period in u, and, making use of the identity $rB_r=\partial\psi/\partial u$, expand around the rational surface $r=r_0$, at which $nq(r_0)-m=0$. With $B_r=b(r)\sin u$, which we might imagine stems from a helical ripple in the plasma current distribution equivalent to $\Delta j_\eta\sim\delta(r-r_0)\cos u$, we find

$$\psi\simeq-\left(\frac{m}{2\pi}\frac{r\langle B_z\rangle}{R}\frac{d\iota}{dr}\right)_{r=r_0}\xi,$$

$$\xi\equiv\tfrac{1}{2}(r-r_0)^2-\Gamma\cos u, \tag{1}$$

$$\Gamma\equiv\left(-\frac{2\pi bR}{m\langle B_z\rangle\, d\iota/dr}\right)_{r=r_0} \tag{2}$$

The island separatrix is given by the $\xi=\gamma^2$ contour, $\gamma\equiv|\Gamma|^{1/2}$, and the full width of the islands is 4γ; see Fig. 1.

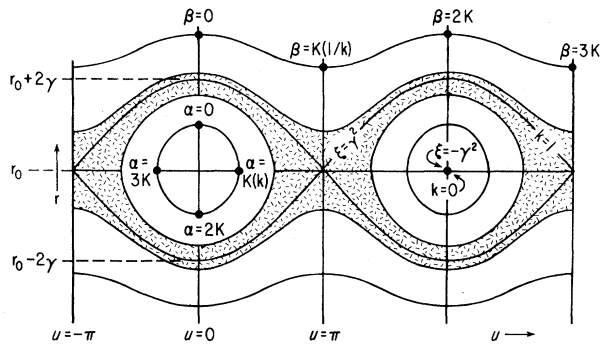

FIG. 1. Structure of primary magnetic islands in the vicinity of $r=r_0$, showing several $\xi=$const contours and, at selected points, values of the angle variables u, α, and β. $\Gamma>0$. Shading indicates a representative region of "braiding," i.e., stochasticity.

With introduction of orthogonal coordinates ξ, α, and η which are local to the primary islands, the coordinate ξ, Eq. (1), parametrizes the magnetic surfaces and $\nabla\xi$ will be everywhere perpendicular to them. The third coordinate, η, is chosen so that $\nabla\eta$ is directed along the $r=$const, $u=$const helical lines and is normalized so that $|\nabla\eta|=1$. $\hat{\alpha}$ is perpendicular to $\hat{\eta}$ and to $\hat{\xi}$, $\hat{\alpha}=\hat{\eta}\times\hat{\xi}$, and we choose to calibrate α so that its rate of change along η is a function of ξ alone, i.e., so that $\dot{\alpha}=d\alpha/d\eta\sim\omega(\xi)$, with the important advantage that Eq. (6), below, will then be immediately soluble by simple Fourier analysis.

One may verify that the choice $d\alpha/du=(d\alpha/d\eta)/(du/d\eta)=\gamma(\partial\xi/\partial r)^{-1}$ will provide that $\omega\sim d\alpha/d\eta$ remains constant along a line of force, i.e., on a single ξ surface. We now introduce new variables, $k(\xi)$,

$$0\leq k^2\equiv(\gamma^2+\xi)/2\gamma^2, \tag{3}$$

and, inside the separatrix, $\zeta(k,u)$, such that $k\times\sin\zeta\equiv\sin(u/2)$. The integration of $d\alpha/du=\gamma(d\xi/dr)^{-1}$ then leads directly to $\zeta=\mathrm{am}(\alpha,k)$ and the coordinate transformation equations, $u=2\sin^{-1}[k\times\mathrm{sn}(\alpha,k)]$ and $r-r_0=2\gamma k\,\mathrm{cn}(\alpha,k)$, where sn and cn are Jacobian elliptic functions, periodic with the period $4K(k)$, $K(k)$ is the complete elliptic integral of the first kind, and am is the inverse function of the elliptic integral of the first kind. The angle variable α increases by the increment $4K(k)$ on one complete circuit (see Fig. 1); if we renormalize this increment to 2π, then the effective rotational transform in the island interior, relative to the local magnetic axis (the elliptic

stagnation point), will be

$$\omega(k)=\frac{2\pi L}{4K(k)}\frac{d\alpha}{d\eta}=\frac{\pi m}{2}\frac{\gamma}{K(k)}\frac{d\iota}{dr}, \tag{4}$$

where $L\equiv 2\pi R[1+(nr_0/mR)^2]^{1/2}$ is the distance along $\langle\vec{B}(r_0,u)\rangle$ for $\Delta z=2\pi R$.

Distances between nearby contours ξ and $\xi+d\xi$ are related by $|d\vec{r}|=d\xi\,|\nabla\xi|^{-1}=2\gamma[\mathrm{cn}^2\alpha+(m\gamma/r_0)^2\times\mathrm{sn}^2\alpha\,\mathrm{dn}^2\alpha]^{-1/2}dk$, and the area inside a closed contour $\xi(k)$, $k\leq 1$, is given by

$$A_i=\frac{16\gamma k(1-k^2)}{|\nabla u|}\frac{dK(k)}{dk}, \tag{5}$$

where $|\nabla u|=mL/2\pi r_0R$. A_i may also be considered the action variable conjugate to the angle variable α; the Hamiltonian would be $\xi(A_i)$.

Outside the separatrix, the appropriate substitution leads to $u=2\,\mathrm{am}(\beta,1/k)$, $r-r_0=2\gamma k\,\mathrm{dn}(\beta,1/k)$, and in (4), $K\to K(1/k)$; see Fig. 1. Distances are related by $|d\vec{r}|=2\gamma[dn^2\beta+(\gamma m/kr_0)^2\,\mathrm{sn}^2\beta\times\mathrm{cn}^2\beta]^{-1/2}dk$, and the total area between the upper and lower $\xi(k)$ contours, $k\geq 1$, from $\beta=0$ to $2K(1/k)$ is $A_0=16\gamma k|\nabla u|^{-1}E(1/k)$, where E is the complete elliptic integral of the second kind.

We now introduce weak asymmetry through the first-order perturbation, $B_r^{(1)}=b^{(1)}\sin w$, $b^{(1)}=\mathrm{const}$, as might be induced by helical plasma-current ripples at an *adjacent* surface, $r=r_1$. The first step is Fourier analysis of the perturbation field, $\sim F^{(1)}$, Eq. (6), into harmonics of the variables α and η. We define λ and κ such that on $r=r_0$, $w=m_1\theta-n_1z/R=\lambda u-\kappa\eta/R$, $\lambda\simeq m_1/m$, $\kappa\simeq n_1-m_1n/m$. The error in the approximate forms for λ and κ is of order $(r_0/qR)^2$. In the ensuing Fourier analysis, 2λ is required to be integral, but the results should be representative of the analysis for other values of λ. The new magnetic surfaces will, near $r=r_0$, be of the form $\varphi^{(0)}(k)+\varphi^{(1)}(k,\alpha,\eta)=\mathrm{const}$, and will satisfy the first-order equation $\vec{B}^{(0)}\cdot\nabla\varphi^{(1)}=(\hat{\eta}B_\eta+\hat{\alpha}B_\alpha)\cdot\nabla\varphi^{(1)}=-\vec{B}^{(1)}\cdot\nabla\varphi^{(0)}$. We approximate B_η as constant, and use Eq. (4) together with $d\alpha/d\eta=|\nabla\alpha|\times B_\alpha/|\nabla\eta|B_\eta$ to evaluate $|\nabla\alpha|B_\alpha$, to find, inside the separatrix,

$$L\frac{\partial\varphi^{(1)}}{\partial\eta}+\frac{4K(k)}{2\pi}\omega(k)\frac{\partial\varphi^{(1)}}{\partial\alpha}=F^{(1)}\frac{d\varphi^{(0)}(\xi)}{d\xi}, \tag{6}$$

$$F^{(1)}\equiv-L\vec{B}^{(1)}(w)\cdot\nabla\xi/B_\eta.$$

Although Eq. (6) was derived for thin primary islands, its use of the action $[A_i(k)$ or $A_0(k)]$ -angle (α) formalism assures us that an equation of this same form could be obtained for thick primary islands.

To solve Eq. (6), we expand both $\varphi^{(1)}$ and $F^{(1)}$ in Fourier series,

$$\varphi^{(1)}=\sum_{\mu,\nu}\varphi_{\mu\nu}(k)\exp\left[i\left(\frac{\pi\mu\alpha}{2K(k)}-\frac{\nu\kappa\eta}{R}\right)\right],$$

and substitute to obtain $\varphi_{\mu\nu}(k)=-iF_{\mu\nu}(k)(d\varphi^{(0)}/d\xi)[\mu\omega(k)-2\pi\nu\kappa]^{-1}$, using $L\simeq 2\pi R$. Since we are free to choose the function $\varphi^{(0)}(k)$, the simplest selection for solubility is $d\varphi^{(0)}/dk=\prod_{\mu,\nu}(k-k_{\mu\nu})$, where $\omega(k_{\mu\nu})=2\pi\nu\kappa/\mu$ for each μ,ν. Then the magnetic surfaces can be determined by expanding $\varphi^{(0)}+\varphi^{(1)}=\mathrm{const}$ around each little resonance, $k=k_{\mu\nu}$:

$$\xi_k\simeq\frac{(k-k_{\mu\nu})^2}{2}-i\left(\mu\frac{d\omega}{dk}\frac{d\xi}{dk}\right)^{-1}\sum_{\pm}F_{\mu\nu}\exp\left[i\left(\frac{\pi\mu\alpha}{2K(k)}-\frac{\nu\kappa\eta}{R}\right)\right], \tag{7}$$

summing just over μ,ν and $-\mu,-\nu$.

To determine $F_{\mu\nu}$, given by

$$F_{\mu\nu}(k)=[8\pi K(k)]^{-1}\int_0^{2\pi}d(\eta\kappa/R)\int_0^{4K}d\alpha\,F(w,k)\exp[i(-\pi\mu\alpha/2K+\nu\kappa\eta/R)]$$

with $F(w,k)\approx-L(b^{(1)}/B_\eta)(r-r_0)\sin(\lambda u-\kappa\eta/R)$, we recall that $r-r_0=2\gamma k\,\mathrm{cn}(\alpha,k)$, $\lambda\simeq m_1/m$, and $u/2\simeq\sin^{-1}(k\,\mathrm{sn}\alpha)\equiv\Omega$. Then we expand, for example for 2λ even, $\sin(\lambda u)=\sin(2\lambda\Omega)=(-1)^{\lambda+1}\times 2^{2\lambda-1}\cos\Omega\sin^{2\lambda-1}\Omega+\ldots=(-1)^{\lambda+1}2^{2\lambda-1}\mathrm{dn}\alpha\,(k\times\mathrm{sn}\alpha)^{2\lambda-1}+\ldots$ and introduce similar expansions for 2λ odd and for $\cos(2m_1\Omega/m)$. Contributions to $F_{\mu\nu}$ from subsequent terms in the series are algebraically small in the expansion parameter, ϵ, Eq. (8). The α integral is easily evaluated if its contour is depressed, for $\mu>0$, to run from $(0,0)$ to $(0,-i\infty)$ to $(4K,-i\infty)$ to $(4K,0)$. Expanding the integrand about the uppermost pair of singular points,[13] we use, for example, near $\alpha=2K-iK'$, $K'\equiv K[(1-k^2)^{1/2}]$, $\mathrm{cn}\alpha=\mathrm{cn}(2K-iK'+\Delta\alpha)=\mathrm{dn}(\Delta\alpha)[ik\,\mathrm{sn}(\Delta\alpha)]^{-1}$, etc., with the expansion parameter ϵ given by

$$\epsilon\equiv\left|\frac{m\gamma\,d\iota/dr}{2\pi\kappa}\right|\approx\left|\frac{m\gamma}{m_1(r_1-r_0)}\right|. \tag{8}$$

(The evaluation of $F_{\mu\nu}$ can be carried through in a straightforward fashion without the small-ϵ expansion—e.g., picking up *all* the residues, etc.

—but the result is cumbersome.) The argument for ω and for the K and K' elliptic integrals is $k_{\mu\nu}$, and $\nu = \pm 1$. r_1 is the radius at which $q(r_1)$ would equal m_1/n_1 if $d\iota/dr$ were constant. In this manner we find $F_{\mu\nu}$ for $\mu > 0$, and for $\mu < 0$ we use $F_{-\mu,-\nu} = F_{\mu\nu}{}^*$. Then Eq. (7) takes the standard form for island contours,

$$\xi_k = \frac{(k-k_{\mu\nu})^2}{2} - \Gamma_k H \cos\left(\frac{\alpha}{\epsilon} - \frac{|\omega\kappa|\eta}{\omega R}\right), \tag{9}$$

$$\Gamma_k \equiv \frac{2^{2\lambda-2}\pi}{(2\lambda)!}\frac{b^{(1)}}{b}\frac{1}{k\,dK/dk}\frac{\exp(-K'/\epsilon)}{\epsilon^{2\lambda-1}},$$

where $H \equiv [\mathrm{sgn}(\omega\kappa)]^{\mu}$. The full width of the little islands in terms of k is $4\gamma_k$, $\gamma_k \equiv |\Gamma_k|^{1/2}$. From the resonance condition $\omega(k_{\mu\nu}) = 2\pi\nu\kappa/\mu$ and using $|\nu| = 1$, we can find the increment in $k_{\mu\nu}$, Δk, corresponding to adjacent resonant surfaces determined by $|\Delta\mu| = 1$. With use of (4) and (8), $\Delta k = 2\pi|\kappa|(\mu^2 d\omega/dk)^{-1} = \pi\epsilon(2\,dK/dk)^{-1}$. Because $\omega(k) \to 0$ as $k \to 1$, Eq. (4), resonances will occur for all integer $\mu > \mu_{\min}$. (A similar pileup also occurs as the separatrix is approached from the outside.) Overlap of little islands will begin when $\Delta k = 4\gamma_k$, which occurs when

$$\sigma \equiv \frac{k}{2\,dK/dk} = \frac{2^{2\lambda+3}}{\pi(2\lambda)!}\frac{b^{(1)}}{b}\frac{\exp(-K'/\epsilon)}{\epsilon^{2\lambda+1}}. \tag{10}$$

For $k \to 1$, $k(2\,dK/dk)^{-1} \approx 1 - k = \delta k$ and $K'(k) \simeq \pi/2$. As noted before, the thickness, δk, of the stochastic layer is given by a nonanalytic function of ϵ, namely, $\sim \epsilon^{-2\lambda-1}\exp(-\pi/2\epsilon)$. For fixed b, ϵ varies as $(d\iota/dr)^{1/2}$ and in this circumstance high-shear regions will be especially susceptible to magnetic braiding. Of some interest also is the steep rise of the function $\epsilon^{-2\lambda-1}\exp(-K'/\epsilon)$ prior to reaching its maximum at $\epsilon = K'/(2\lambda+1)$. In this range a modest increase in ϵ can produce a sudden large increase in the thickness of the braiding layer.

Outside of the zero-order separatrix, the expressions for ω and ϵ are the same as before except that $K = K(1/k)$, etc. Equations for the new magnetic surfaces in the neighborhood of $k = k_{\mu\nu}$ are in the form of set (9) but with $\alpha \to \beta$, $(k\,dK/dk)^{-1} \to -k^{2\lambda}[dK(1/k)/dk]^{-1}$ and $H \to \frac{1}{2}[1 + (-1)^{\mu+2\lambda}] \times [1 + \mathrm{sgn}(\omega\kappa)]$. Resonances appear only for $\mathrm{sgn}(\omega\kappa) > 0$ and $|\Delta\mu| = 2$, so that the density of little islands and the thickness of the braiding layer are reduced to approximately half their inside-separatrix values. The expression for the overlap condition resembles (10) except that the new left-hand side reads $[k^{2\lambda}dK(1/k)/dk]^{-1} \sim 2\delta k$.

Using the results of the previous paragraphs together with the expression for A_i, Eq. (5), and for A_0, we can easily derive an expression for the ratio of the total stochastic area both inside and outside the primary separatrix, δA, to the total area, A, within the primary separatrix, valid for $\sigma \ll 1$,

$$\delta A/A \simeq 0.75\sigma\ln(27.4/\sigma). \tag{11}$$

The considerations here can be applied to study the effect of toroidal geometry on magnetic islands. To first order in r/R, the axisymmetric poloidal and toroidal fields are given[14] by $B_p(\psi) \times [1 + (r/R)\Lambda(\psi)\cos\theta]$ and $B_t(\psi)[1 - (r/R)\cos\theta]$; the quantity $\Lambda + 1$ is proportional to the magnitude of the effective "vertical" field needed to balance the well-known toroidal hoop forces. We compute the excitation function $F = \pi\gamma^2 n(\Lambda+1)(r/R) \times \{\sin[(m+1)\theta - nz/R] + \sin[(m-1)\theta - nz/R]\}$, and carry out the perturbation analysis as before to find, with $m_1 = m \pm 1$, $n_1 = n$,

$$\frac{k}{2\,dK/dk} = \left|\frac{mr(\Lambda+1)}{\pi R}\right|\frac{2^{2\lambda+1}}{(2\lambda-1)!}\frac{\exp(-K'/\epsilon)}{\epsilon^{2\lambda+1}}, \tag{12}$$

as a measure of the beginning of little-island overlap and magnetic braiding just inside the separatrix.

Abel inversions of x-ray intensity oscillations from the ST tokamak indicated,[9] just prior to disruption, the presence of a magnetic island near the $q = 2$ surface of $4\gamma = 3.5$–4 cm full thickness. With use of $m = 2$, $n = 1$, $r_0 = 8$ cm, $R = 109$ cm, $d\iota/dr = 0.4$ cm^{-1}, and thus $\epsilon = 0.24$ and $\lambda = \frac{3}{2}$, and with $\Lambda = 0$, simultaneous solution of Eqs. (5) and (12) shows that $\sim 30\%$ of the interior area of the $m = 2$ island would be braided by the toroidal perturbation of the symmetry, close to the maximum of (12) with respect to variation of ϵ.

It is a pleasure to acknowledge the help of Dr. S. Cohen, Dr. J. Ehrman, Dr. J. Finn, Dr. M. N. Rosenbluth, and Dr. S. von Goeler.

*This work was supported by the U. S. Energy Research and Development Administration (formerly U. S. Atomic Energy Commission), under Contract No. E(11-1) 3073.

[1]H. P. Furth, J. Killeen, and M. N. Rosenbluth, Phys. Fluids 6, 459 (1963).

[2]H. P. Furth, P. H. Rutherford, and H. Selberg, Phys. Fluids 16, 1054 (1973).

[3]S. von Goeler, in *Proceedings of the Seventh European Conference on Controlled Fusion and Plasma Physics, Lausanne, Switzerland, 1975* (European Physical

Society, Geneva, Switzerland, 1975).
[4]D. W. Kerst, J. Nucl. Energy, Part C 4, 253 (1962).
[5]P. H. Rutherford, Phys. Fluids 16, 1903 (1973).
[6]B. V. Waddell, D. A. Monticello, M. N. Rosenbluth, and R. B. White, Bull. Am. Phys. Soc. 20, 1342 (1975).
[7]T. H. Stix, Phys. Rev. Lett. 30, 833 (1973).
[8]H. Grad, Phys. Fluids 10, 137 (1967).
[9]M. N. Rosenbluth, R. Z. Sagdeev, J. B. Taylor, and G. M. Zaslavskii, Nucl. Fusion 6, 297 (1966).
[10]N. N. Filonenko, R. Z. Sagdeev, and G. M. Zaslavsky, Nucl. Fusion 7, 253 (1967).
[11]G. M. Zaslavskii and N. N. Filonenko, Zh. Eksp. Teor. Fiz. 54, 1590 (1968) [Sov. Phys. JETP 27, 851 (1968)]. See also G. M. Zaslavskii and B. V. Chirikov, Usp. Fiz. Nauk 105, 3 (1971) [Sov. Phys. Usp. 14, 549 (1972)].
[12]J. L. Johnson, C. R. Oberman, R. M. Kulsrud, and E. A. Frieman, Phys. Fluids 1, 281 (1958).
[13]See, for example, E. Jahnke and F. Emde, *Tables of Functions* (Dover, New York, 1945), 4th ed., Chap. VI.
[14]V. D. Shafronov, in *Reviews of Plasma Physics*, edited by M. A. Leontovich (Consultants Bureau, New York, 1966).

Distribution of Self-Generated Current in Laser-Produced Plasmas

M. G. Drouet and R. Bolton
Direction Sciences de Base, Institut de Recherche de l'Hydro-Québec, Varennes, Québec, Canada, J0L 2P0
(Received 18 December 1975)

The current associated with the self-generated magnetic field has been measured in air and nitrogen at various pressures in a 4-J, 30-nsec-Nd-laser-produced plasma using a fast probe embedded in the copper target. The results reveal an active participation of the target in the current-flow process with anodic and cathodic regions, the source of the current (magnetic field) being at the plasma-target interface.

Although the existence of large self-generated magnetic fields in laser-produced plasmas has been well established experimentally[1-3] and their origin considered in a large number of theoretical papers,[4-6] the currents associated with these fields have only been determined by applying $\nabla \times \vec{B} = \mu_0 j$ to the magnetic field data.[2] We present here direct measurements, resolved in space and time, of the distribution of current flow to and from a target irradiated by a focused Nd-glass laser beam.

Our experiments were conducted in both air and nitrogen at various pressures. The beam from a Nd-glass laser ($\lambda = 1.06$ μm) was focused at normal incidence upon a flat copper target in an experimental chamber. The laser pulse was 4 J, 30 nsec (full width, half-energy). The focal-spot diameter at the target surface (in the absence of plasma), with a 10-cm lens, was 250 μm at half-energy, giving a power density of approximately 10^{11} W/cm^2.

The current flow through the plasma-target interface was monitored, as shown in Fig. 1, using a small wire probe (0.32 mm o.d.) embedded in the target and insulated from it except at its end where it is soldered to it. The wire probe is terminated in the form of a loop so as to inductively couple the element of current incident on the probe surface to a small secondary coil. The transfer impedance of this arrangement is a mutual inductance, the high-frequency response being limited by a pole because of the combination of the total output inductance and the 50-Ω termination. The experimental values are 4×10^{-9} H for the transfer inductance and 4 nsec (max) for the equivalent time constant of the pole. Therefore, by using this probe technique, direct oscilloscope display of dI/dt, the time rate of change of the net current flow I through the probe-plasma interface, is achieved. A notable advantage

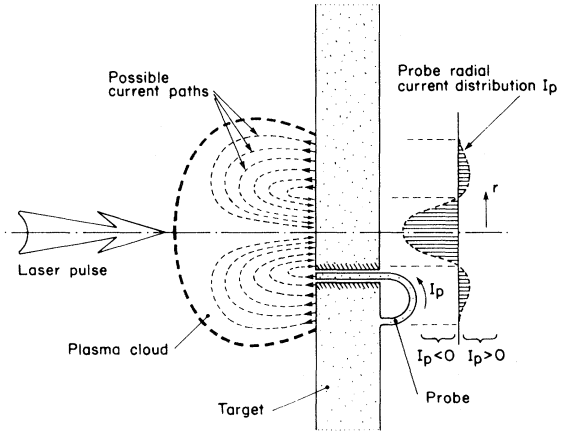

FIG. 1. Diagram showing the target with the wire probe sampling part of the current flow through the plasma-target interface.